

Protein-S-nitrosylation of human cytomegalovirus pp65 reduces its ability to undermine cGAS

Justin B. Cox,¹ Masatoshi Nukui,¹ Eain A. Murphy¹

AUTHOR AFFILIATION See affiliation list on p. 16.

ABSTRACT Post-translational modifications (PTMs) are key regulators of various processes important for cell survival. These modifications are critical for dealing with stress conditions, such as those observed in disease states, and during infections with various pathogens. We previously reported that during infection of primary dermal fibroblasts, multiple human cytomegalovirus (HCMV)-encoded proteins were post-translationally modified by the addition of a nitric oxide group to cysteine residues, a modification called protein-S-nitrosylation. For example, tegument protein pp71 is nitrosylated, diminishing its ability to inhibit STING, a protein necessary for DNA virus immune response. Herein, we report that an additional HCMV tegument protein, pp65, responsible for the inhibition of cGAS is also modified by protein-S-nitrosylation on two cysteine residues. Utilizing site-directed mutagenesis to generate recombinant viruses that encode a pp65 that cannot be protein-S-nitrosylated, we evaluated the impact of this PTM on viral replication and how the virus impacts the cGAS/STING pathway. We report that the nitrosylation of pp65 negatively impacts its ability to block cGAS enzymatic functions. pp65 protein-S-nitrosylation mutants demonstrated a decrease in cGAS/STING-induced IRF3 and TBK1 phosphorylation. Additionally, we observed a reduction in IFN- β 1 secretion in NuFF-1 cells expressing a nitrosylation-resistant pp65. We report that HCMV expressing a protein-S-nitrosylation-deficient pp65 is resistant to the activation of cGAS in the infection of primary dermal fibroblasts. Our work suggests that nitrosylation of viral proteins may serve as a broadly neutralizing mechanism in HCMV infection.

IMPORTANCE Post-translational modifications (PTM) are utilized by host cells to limit an invading pathogen's ability to establish a productive infection. A potent PTM, called protein-S-nitrosylation, has anti-bacterial and anti-viral properties. Increasing protein-S-nitrosylation with the addition of nitric oxide donor compounds reduced HCMV replication in fibroblasts and epithelial cells. We previously reported that protein-S-nitrosylation of HCMV pp71 limits its ability to inhibit STING. Herein, we report that the protein-S-nitrosylation of HCMV pp65 impacts its ability to limit cGAS activity, an additional protein important in regulating interferon response. Therapeutically, patients provided nitric oxide by inhalation reduced viral replication in coronavirus disease 2019, influenza, and even impacted bacterial growth within patients' lungs. It is thought that an increase in free nitric oxide increases the frequency of nitrosylated proteins. Understanding how protein-S-nitrosylation regulates a common DNA virus like HCMV will provide insights into the development of broadly neutralizing therapeutics in drug-resistant viral infections.

KEYWORDS protein-S-nitrosylation, HCMV, pp65, herpesviruses, cGAS, STING, PTM

Human cytomegalovirus (HCMV), a large ubiquitous beta-herpesvirus, is endemic in the human population (1, 2). Upon infection with HCMV, the virus persists for the

Editor Derek Walsh, Northwestern University
Feinberg School of Medicine, Chicago, Illinois, USA

Address correspondence to Eain A. Murphy,
murphye1@upstate.edu.

The authors declare no conflict of interest.

See the funding table on p. 16.

Received 14 March 2025

Accepted 20 March 2025

Published 17 April 2025

Copyright © 2025 Cox et al. This is an open-access
article distributed under the terms of the [Creative
Commons Attribution 4.0 International license](#).

lifetime of the host, as the virus has the capacity to establish a latent infection within myeloid progenitor cells coupled with sporadic reactivation, resulting in lytic replication in various cell types (3, 4). It is estimated that 30–80% of adults are HCMV-seropositive, and, typically, a competent immune system renders lytic reactivations asymptomatic (5, 6). However, in immunocompromised individuals, such as bone marrow and HIV-positive patients, HCMV often results in severe disease and death (7, 8). Equally problematic are HCMV infections in neonates with underdeveloped immune systems. HCMV is currently the leading cause of congenital infections and responsible for cognitive and physical birth defects, such as hydrocephaly and microcephaly in newborns if the mother contracts a primary HCMV infection while pregnant (9). Currently, there is no vaccine for HCMV, thus making therapeutic interventions for pre-existing infections a focus for limiting infection spread. While direct-acting antiviral drugs have proven effectual for controlling HCMV infection, they are becoming less clinically effective, as resistant strains of the virus have emerged (10, 11). Thus, identifying how the innate and intrinsic immune responses limit HCMV infection and characterization of PTMs that undermine viral virulence factors is essential in developing novel neutralizing therapeutics.

Innate immunity is one of the earliest steps in combating viral and bacterial infections. Pathways involved in this recognition are responsible for identifying pathogen-associated molecular patterns (PAMPs) within the cytoplasm of a cell. The recognition of PAMPs, such as cytoplasmic dsDNA, by pattern recognition receptors like the cyclic guanine-adenosine synthase (cGAS) enzyme is essential for controlling DNA virus infections (12–15). Once cGAS encounters cytoplasmic dsDNA, it facilitates the enzymatic reaction fusing ATP and GTP, thereby generating guanosine-adenosine 2'3'-cyclic monophosphate (2'3'-cGAMP), an agonist for stimulator of interferon genes (STING) (12, 16–21). Stimulation of cGAS results in the potent inhibition of viruses, such as HCMV (22–24). However, HCMV encodes various proteins that function to undermine cellular DNA sensors, such as STING and cGAS (6, 25). Packaged in the tegument of HCMV is pp65, a protein encoded by open reading frame Unique Long 83 (UL83) (26). The direct interaction of pp65 and cGAS decreases the latter's ability to produce 2'3'-cGAMP, thus reducing STING-mediated immunity and interferon response (26, 27). Underscoring its importance during the initial stages of viral infection, pp65 comprises approximately 15% of the tegument of infectious virions and most of the approximate weight of dense bodies (28).

Intrinsic immunity not only detects and responds to foreign substances, it also functions to induce modifications in viral proteins leading to a reduction in the protein's activity. A cell typically modifies the biological functions of proteins through PTMs, such as modifications that may lead to protein degradation, thus limiting their presence within an infected cell. Modifications, such as ubiquitination, SUMOylation, and phosphorylation, can each serve as innate immune mechanism for infected cells for virally infected cells (29–33). One such modification that remains understudied due to its liable nature is called protein-S-nitrosylation. This modification involves a nitric oxide group being attached to the thiol group within a cystine amino acid (34). This modification can result in multiple consequences such as controlling di-sulfide linkages, altering enzymatic activity, and functioning in anti-viral properties (34–39). Zell et al. observed that the active sites of the 2A and 3C proteases of coxsackie B3 virus are protein-S-nitrosylated, and as a result, this PTM impacts their proteolytic functions (39). The anti-viral functions of protein-S-nitrosylation of viral proteins are a novel cellular mechanism that cells can use to limit the functions of the target protein.

We previously reported that protein-S-nitrosylation of HCMV pp71 inhibits its ability to attenuate STING. As we observed that pp65 also is modified in a similar fashion, coupled with the fact that it is involved in the cGAS/STING pathway, we wanted to investigate the impact of protein-S-nitrosylation on this protein. Herein, we report that pp65 constructs, in which the identified protein-S-nitrosylated cysteines were changed to structurally related serines, inhibit cGAS with better efficiency, suggesting

that the PTM is inhibitory to the viral protein functions. Furthermore, we observed that a double-mutant pp65 (DM-pp65) that is not protein-S-nitrosylated has a growth advantage over wild-type (WT) pp65 in the presence of a potent cGAS agonist, G3-YSD. These data suggest that protein-S-nitrosylation is not just a singular anti-viral mechanism but functions as a broadly neutralizing mechanism to improve the function of the cGAS/STING pathway.

RESULTS

Human cytomegalovirus pp65 is nitrosylated in HCMV infection

Our previous work utilized mass spectrometry to identify peptides that contain a protein-S-nitrosylated cystine during HCMV infection of human newborn foreskin fibroblasts (NuFF-1) and identified 13 HCMV proteins that contained this PTM (40). One of these identified proteins was pp65, a tegument protein critical for undermining host innate immune responses. Our analysis results indicated that pp65 is nitrosylated at cysteine residues 276 and 306 (Fig. 1A). To validate the protein-S-nitrosylation status of pp65 and characterize the kinetics of when the PTM is added to pp65, human NuFF-1 cells were infected with HCMV at a multiplicity of infection (MOI) of 1, and cell lysates were collected in non-reducing conditions to preserve the protein-S-nitrosylation modification at 24, 48, and 72 hpi. Equal amounts of infected NuFF-1 cell lysates were subjected to a biotin switch assay, in which this reaction covalently links a biotin moiety on protein-S-nitrosylated cysteine amino acids in any given protein allowing affinity purification with avidin beads. Total biotinylated protein was affinity-purified, followed by immunoblot analysis with anti-pp65 and anti-actin antibodies. Actin was specifically

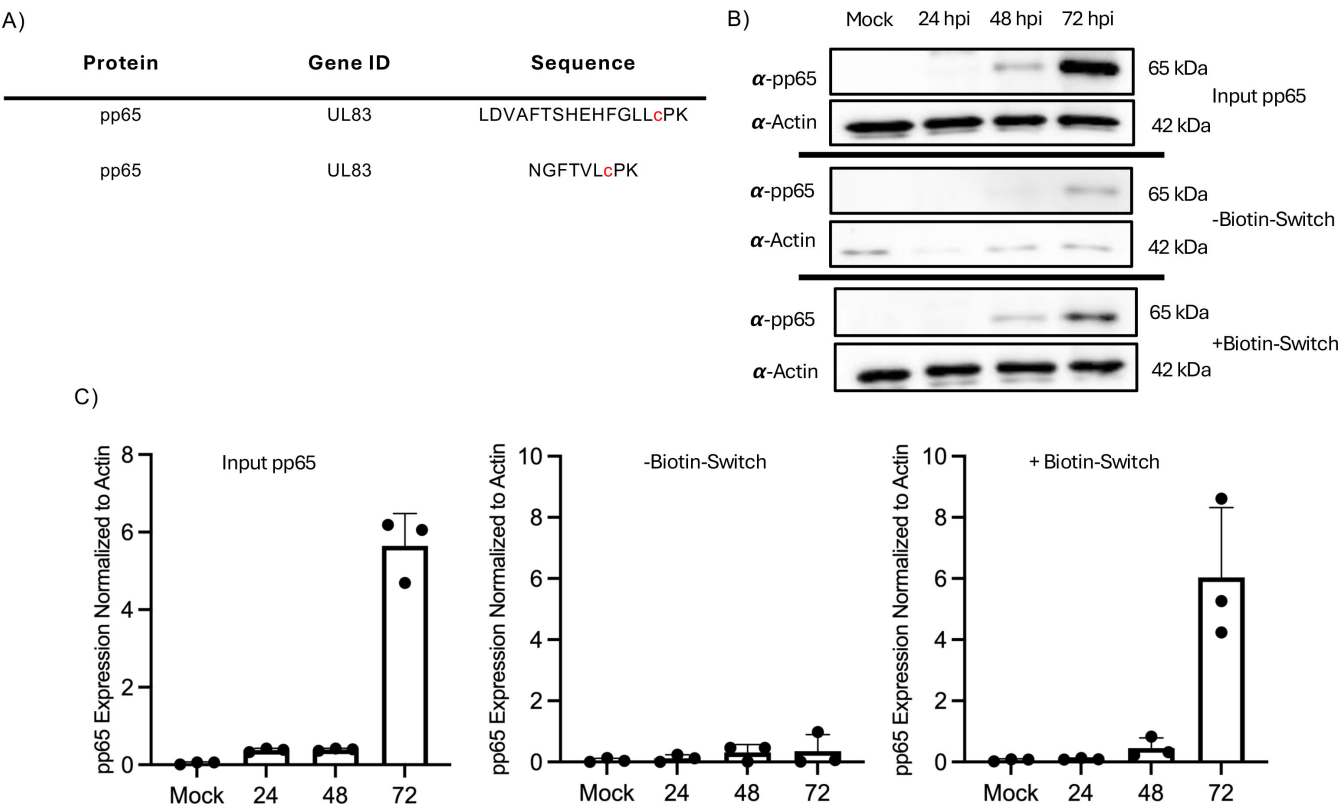


FIG 1 HCMV pp65 is protein-S-nitrosylated in infection of primary dermal fibroblasts. (A) Proteomic analysis of HCMV-infected fibroblast lysates 96 hpi identified specific sites of pp65 that are protein-S-nitrosylated (40). (B) NuFF-1 cells were infected at an MOI of 1 for 24, 48, and 72 hpi, and 100 µg of protein was subjected to a biotin switch, and then affinity purified with streptavidin beads. Biotinylated protein was separated by SDS-PAGE, transferred to a nitrocellulose membrane, and immunoblotted with primary antibody to pp65. A representative result of three biological repeats is shown. (C) Band intensities for pp65 expression in the input, -biotin switch, and +biotin switch groups were measured for panel B, and all samples were normalized to actin. *n* = 3.

chosen as a suitable control, as it has been reported to be protein-S-nitrosylated (41–44). Our results show that as early as 48 h post-infection (hpi), pp65 is nitrosylated with increasing levels of the PTM being observed at 72 hpi (Fig. 1B), validating the results of the tandem mass spectrometry (MS/MS) analysis that pp65 is nitrosylated during the course of a lytic HCMV infection, and the modification is observed with similar kinetics and levels as the protein expression of pp65. To quantitate these results, band intensity was measured and confirmed the findings from the western blotting results (Fig. 1C).

Nitrosylation-deficient pp65 expressing HCMV replicates with similar kinetics compared to WT virus

To determine if protein-S-nitrosylation impacts the biological functions of the viral protein, we generated a nitrosylation-deficient pp65, termed DM-pp65, where each of the two identified protein-S-nitrosylated cystines C276/C306 were mutated to the structurally similar amino acid serine, which is identical to cystine, except for the absence of a sulfur atom, thus rendering it a non-suitable substrate for the modification. In addition, we generated single mutants (SM) for each of the individual sites (Fig. 2A). As recombinering may cause spurious off-site mutations to arise, thereby confounding potential results, we generated a revertant of our mutant DM-pp65 virus so that the two mutated serines are reverted back to the original cysteines, termed Rev-pp65. To determine if DM-pp65 exhibits an altered growth kinetics when compared to WT or Rev-pp65 virus, NuFF-1 cells were infected at an MOI of 1.0, and the cell-free virus was collected on 0, 3, 5, and 7 days post-infection (dpi). A fraction of inoculum was saved to confirm the initial starting titer for infection. Viral titers were then quantified by TCID50 analysis. Viral titers of WT, DM-pp65, and Rev-pp65 virus exhibited similar growth kinetics suggesting that the mutations had little impact on the ability of the virus to undergo lytic replication in fibroblasts (Fig. 2A).

To further confirm growth kinetics of NuFF-1, a multi-step growth curve was done for WT-pp65, DM-pp65, and Rev-pp65, allowing multiple rounds of replication for all viral groups. NuFF-1 cells were infected at an MOI of 0.1, and the cell-free virus was collected at 0, 3, 6, 9, 12, and 15 dpi. Inoculum was stored in this group as well to confirm initial titers. All time points and the inoculum were analyzed by TCID50. The viral titers for WT, DM-pp65, and Rev-pp65 were similar and followed the same growth kinetics as a single-step growth curve (Fig. 2B). This further suggests that the mutations did not impact the ability of the virus to replicate in lytic infection of fibroblasts.

Next, we wanted to evaluate the protein kinetics of pp65 expression in WT and DM-pp65. pp65 is a viral late transcript with observable *de novo* expression initiating at 24 h post-infection and highest expression observed late in infection (45–47). To compare the *de novo* expression of WT and DM-pp65 NuFF-1 cells were infected at an MOI of 1, and cell lysates were collected at 24, 48, and 72 HPI. Protein expression was then measured by immunoblot. At each time point, we observed similar levels of pp65 protein expression from the WT and DM-pp65 viruses, suggesting that the mutations did not impact the levels of pp65 protein expression or the timing of their translation (Fig. 2C).

pp65 is a major tegument protein important in the initial stages of infection and represents up to 15% of the mass of an infectious virion (48). To determine if protein-S-nitrosylation impacts the loading of pp65 into the tegument of HCMV, NuFF-1 cells were infected at an MOI of 1.0 with WT and DM-pp65, and lysates were collected at 6 hpi, a time point prior to the *de novo* synthesis of pp65. Lysates were then collected, and deposition of tegument delivered pp65 was analyzed by immunoblot. We observed similar band intensities in both WT and DM-pp65 conditions, suggesting that loading and/or delivery of pp65 is not impacted by the substitutions of serine for cystines in pp65 (Fig. 2D). In summary, the substitution of serine for protein-S-nitrosylated cystine did not alter the replication kinetics or tegument loading of pp65 in fibroblasts.

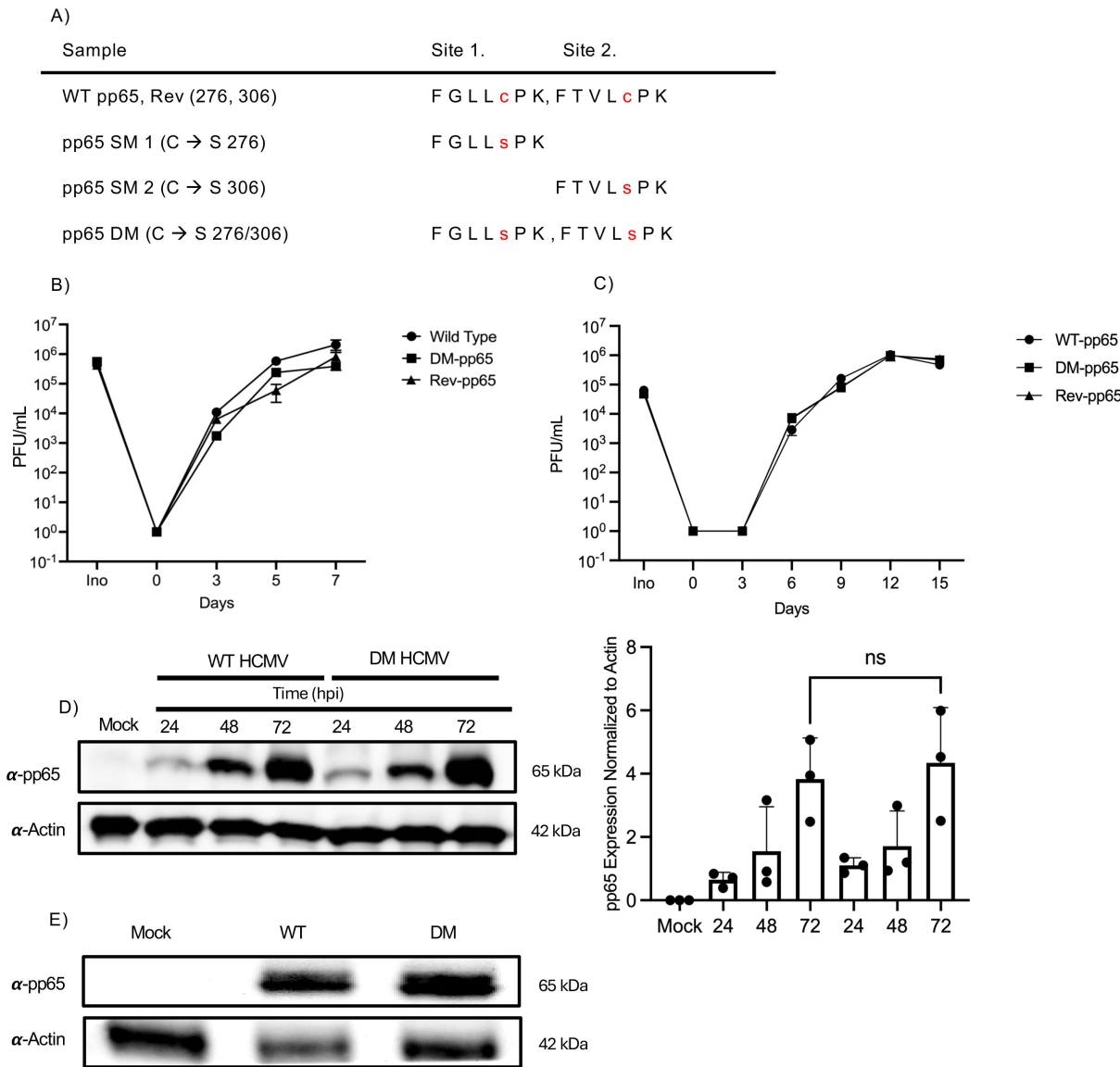


FIG 2 Nitrosylation-deficient pp65 expressing HCMV replicates with similar kinetics to WT virus. (A) Table representing the mutations made in all HCMV mutant viruses. WT virus is denoted as C276/C306, SM1-pp65 C276S, SM2-pp65 C306S, and DM-pp65 C276S/C306S. (B) NuFF-1 cells were infected at an MOI of 1 with WT, DM, or Revertant HCMV, and the supernatant was collected on days 0, 3, 5, and 7 dpi. Viral titers were measured by TCID50 with mCherry expression. The inoculum was saved to determine equal PFU upon infection of NuFF-1 cells. (C) NuFF-1 cells were infected at an MOI of 0.1 with WT-pp65, DM-pp65, and Rev-pp65, and cell-free virus was collected at days 0, 3, 6, 9, 12, and 15 dpi. Viral titers were measured by TCID50 with mCherry expression. Inoculum was saved to determine equal PFU upon infection of NuFF-1 cells. (D) NuFF-1 cells were infected with WT or DM pp65 at an MOI of 1, and cell lysates were collected at 0, 24, 48, and 72 hpi. Protein lysates were immunoblotted with primary antibody to pp65 and actin. A representative western of three biological replicates is shown with quantification of all three experiments shown to the right. (E) NuFF-1 cells were infected at an MOI of 1 with WT or DM-pp65 HCMV for 6 h. Protein lysates were immunoblotted with primary antibody to pp65 and actin. (B–E) $n = 3$.

DM-pp65 HCMV replication is more resistant to G3-YSD treatment

A key biological function of pp65 is to bind to and inhibit the activity of cGAS (26). We, therefore, focused our efforts on evaluating the impact of protein-S-nitrosylation of pp65 in the context of the cGAS/STING pathway, as we have previously reported that protein-S-nitrosylation of another HCMV tegument protein, pp71, reduced its ability to inhibit the biological functions of the STING protein. cGAS upon engagement with cytoplasmic dsDNA produces 2'3'-cGAMP, which in turn stimulates STING to initiate interferon and pro-inflammatory cytokine transcriptional induction. To activate cGAS, we treated cells

with a cGAS agonist, G3-YSD, that was introduced into cells by lipid-based transfection. We monitored cell viability upon treatment of G3-YSD using a WST viability assay. Cell viability remained consistent with no significant reduction of viability observed from 0.4 to 0.8 μg of G3-YSD. No toxicity was observed. No significant toxicity was observed in the vehicle group, which was just lipofectamine. However, there was a significant reduction in cell viability at 1.6 μg of G3-YSD with a cell viability of approximately 83% (Fig. 3A). Using a cGAS agonist, G3-YSD, we observed a dose-dependent inhibition of HCMV virion production following treatment with G3-YSD at concentrations that did not alter cellular viability, highlighting the role of activated STING in establishing an antiviral state (Fig. 3B). Since decreases in viral titers were identified in WT HCMV infection, we wanted to investigate how protein-S-nitrosylation-deficient HCMV DM-pp65 replicates in the presence of an activated anti-viral state. NuFF-1 cells were pre-transfected with 0.4, 0.8, and 1.6 μg of G3-YSD or just vehicle, as 1.6 μg of G3-YSD was sufficient in reducing WT HCMV viral titers below the limit of detection. NuFF-1 cells were then infected at an MOI of 0.1 with WT or DM-pp65 HCMV, with media collected 7 dpi and titers measured by the TCID₅₀ assay. As expected, percent viral titer decreased in WT HCMV infection at all concentrations of G3-YSD, as seen in Fig. 3B. In the DM-pp65-infected cells, there was no significant decrease in viral titers treated with 0.4 and 0.8 μg of G3-YSD (Fig. 3C). However, a significant decrease in percent viral titers in the 1.6 μg treatment group did attenuate DM-pp65 replication by 50% but not below the limit of detection like WT HCMV. These data suggest that protein-S-nitrosylation-deficient DM-pp65 can antagonize cGAS, even in an activated state, whereas WT HCMV infection is inhibited.

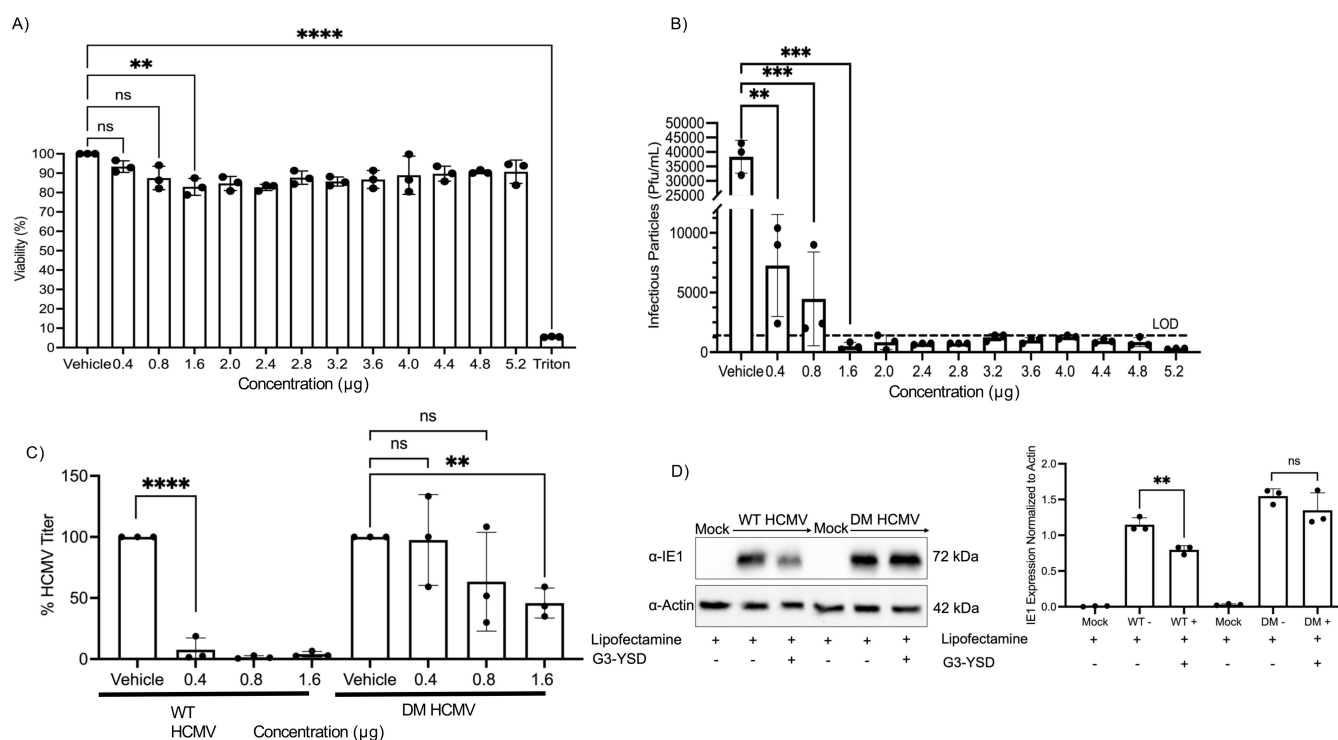


FIG 3 Nitrosylation-deficient pp65 is resistant to G3-YSD treatment. (A) WST assay of NuFF-1 cells transfected with G3-YSD 24 h after transfection. NuFF-1 cells were transfected for 6 h, with media removed, and 24 h later subjected to the WST assay to measure mitochondrial activity. WST-1 solution was added to each well and incubated for 2 h at 37°C. Following this, the absorbance of each well was measured at 420 nm. 10% Triton X-100 was used as a control to observe cell death within the assay. (B) NuFF-1 cells were transfected with G3-YSD for 6 h with indicated concentrations, and then infected with WT HCMV 24 h later at an MOI of 0.1. Viral titers were measured by TCID₅₀ assay 7 days post-infection and reported as PFU/mL. (C) NuFF-1 cells were transfected with 0.4, 0.8, and 1.6 μg of G3-YSD for 6 h, and then 24 h later infected with WT or DM-pp65 at an MOI of 0.1. All viral titers were measured 7 days post-infection by TCID₅₀ assay. (D) NuFF-1 cells were transfected with 0.8 μg of G3-YSD for 2 h, and then infected with WT-pp65 HCMV or DM-pp65 HCMV at an MOI of 1.0. 24 hpi protein lysates were collected and immunoblotted with primary antibody to IE1, and then incubated with a secondary anti-mouse antibody. Densitometry of IE1 expression is included for comparisons of IE1 expressions from the western blots. (A–) $n = 3$, $P < 0.01$ **, $P < 0.001$ ***, and $P < 0.0001$ ****.

This result would lead one to hypothesize that DM-pp65 may be degrading cGAS or that the protein-S-nitrosylation of pp65 may cause a reduced interaction, causing a stronger interaction between cGAS and DM-pp65.

cGAS is not degraded during infection of NuFF-1 cells with either WT or DM-pp65

DM-pp65 demonstrates increased resistance to cGAS activation, as noted from its ability to replicate in the presence of G3-YSD with a possible explanation that the protein levels of cGAS are regulated by pp65. To determine if cGAS is degraded in WT or DM-pp65 HCMV infection, NuFF-1 cells were infected at an MOI of 1 with WT and DM-pp65, and lysates were collected at 12, 24, 48, and 72 hpi. Immunoblots using cGAS-specific antibodies indicated that in both the WT and DM-pp65-infected NuFF-1 cells, degradation of cGAS was not observed at any of the time points of infection (Fig. 4). This was in line with previous reports that cGAS is not degraded during HCMV infections, where wild-type pp65 is expressed (26). These data suggest that the resistance observed in DM-pp65 HCMV is not from the degradation of cGAS but possibly from the limitation of the activity of cGAS with better efficiency than a WT pp65.

Wild-type and DM-pp65 interact with cGAS with similar efficiencies

The data thus far support a model in which the nitrosylation of pp65 may serve as an anti-viral property due to its reduced capacity to block the activation of the STING pathway in the presence of G3-YSD. However, it is critical to understand the biological impact of pp65 when protein-S-nitrosylation of the protein is inhibited. To test this, we generated stable cell lines that express three nitrosylation-resistant pp65 mutants SM1-pp65, SM2-pp65, and DM-pp65. We only determined if WT-pp65 stable cell lines are protein-S-nitrosylated by biotin switch assay, as SM1 and SM2 still have cysteines that can be protein-S-nitrosylated. As expected, immunoblotting identified a band in the avidin-purified group that underwent the biotin switch. This suggests that pp65 is still protein-S-nitrosylated in stable cell lines without the presence of other viral factors and viral DNA (Fig. 5A).

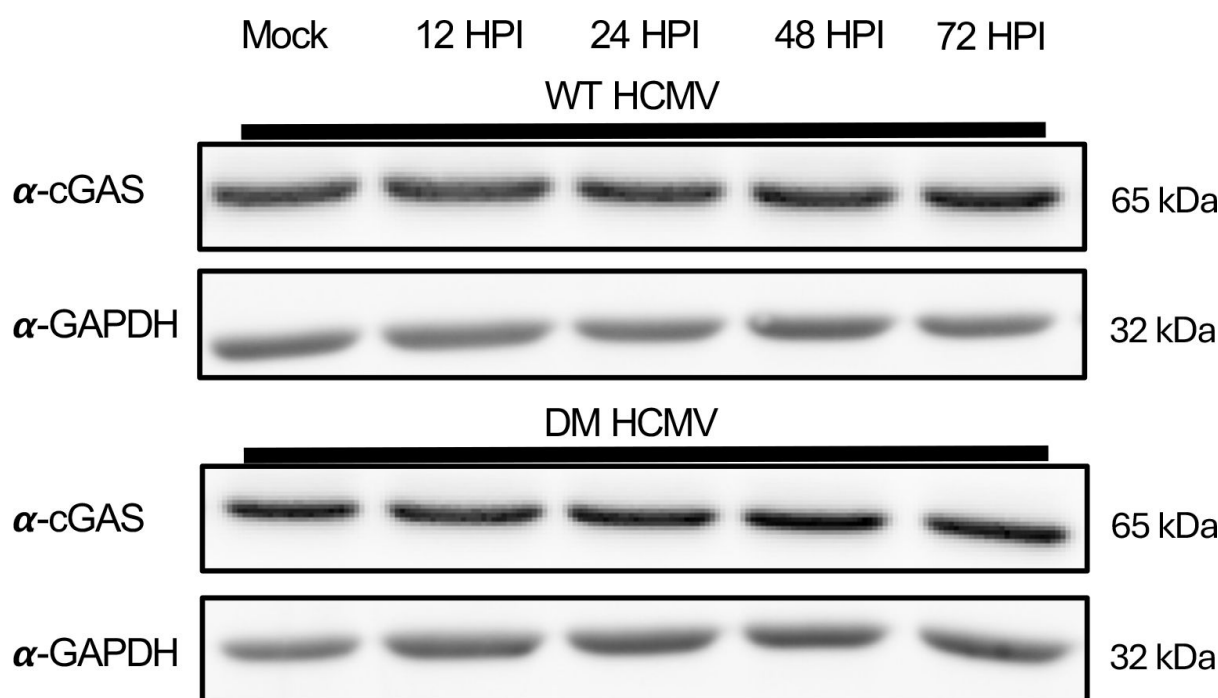


FIG 4 Expression levels of cGAS are unaffected by infection by WT and DM HCMV. NuFF-1 cells were infected with HCMV WT or DM-pp65 at an MOI of 1, and cell lysates were collected at 12, 24, 48, and 72 hpi. Protein lysates were immunoblotted with primary antibody to pp65 and GAPDH. $n = 3$.

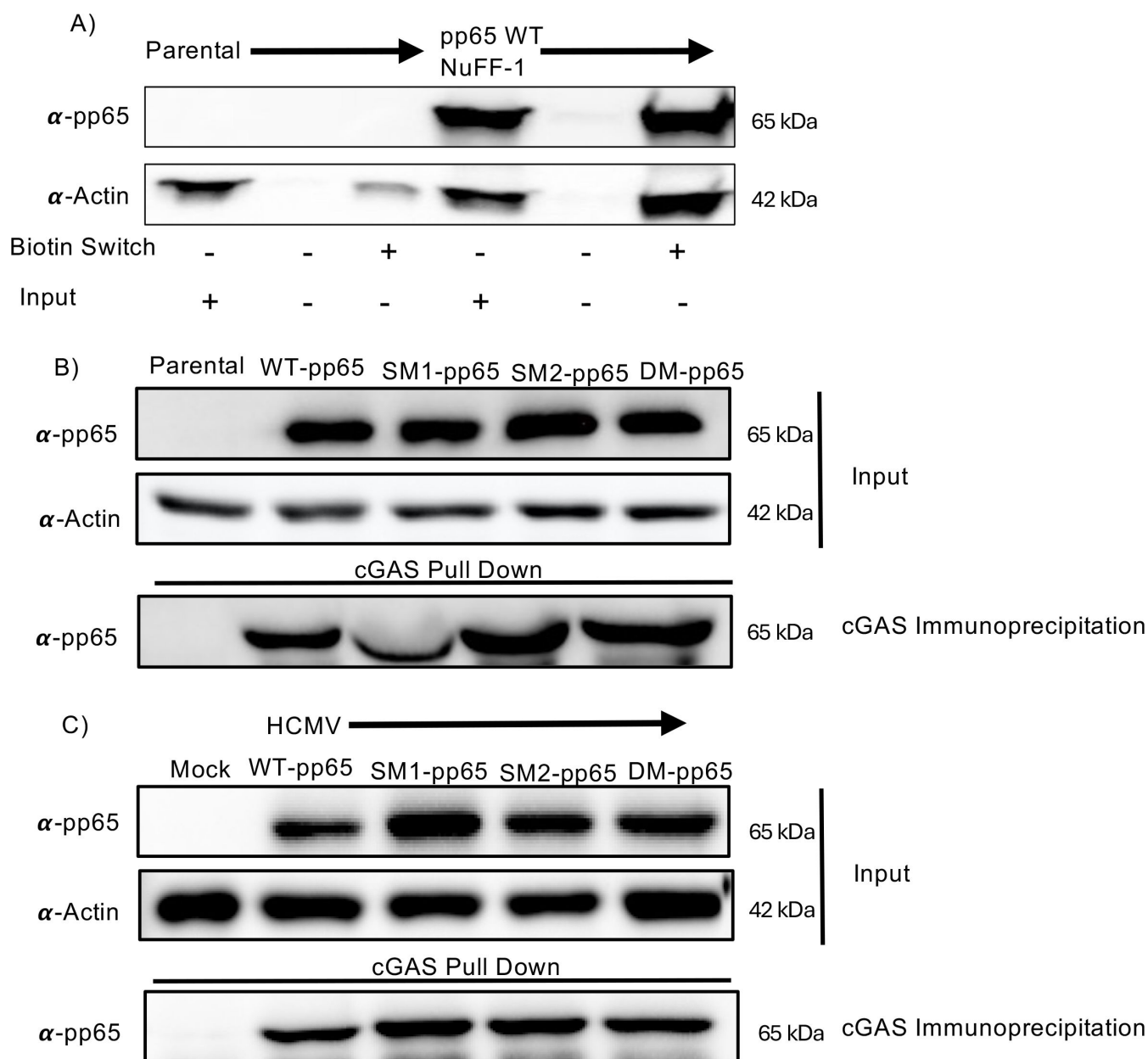


FIG 5 HCMV pp65 mutants interact with cGAS in stable cell lines and infection. (A) NuFF-1 parental and pp65 WT expressing NuFF-1 cells were lysed using the protein-S-nitrosylation detection kit. Following cell lysis, 100 μ g of protein cell lysate underwent the "biotin switch" reaction following the manufacturer's instructions. Following the biotin switch, all reactions were affinity purified with avidin-coated beads. Protein was then separated to 8% SDS-PAGE and blotted with primary antibody specific to pp65. (B) Stable cell lines expressing WT pp65 (C276/C306), SM1-pp65 (C276S), SM2-pp65 (C306S), and DM-pp65 (C276S/C306S) were lysed with Co-IP lysis buffer and incubated with anti-mouse dynabeads. Protein was separated by 8% SDS-PAGE, and 5 μ g of input lysate was used to confirm expression of the pp65 protein. The membrane was immunoblotted with pp65 antibody to confirm pulldown from interacting with cGAS. Actin was used to confirm equal loading of input. (C) NuFF-1 cells were infected at an MOI of 3 for 72 h with WT and all pp65 nitrosylation-deficient mutants. Cells were lysed with Co-IP lysis buffer, and protein was incubated with cGAS-coupled dynabeads overnight at 4°C. Next, 5 μ g of input was separated to confirm equal expression of pp65 in each reaction. Isolated proteins were separated by SDS-PAGE, transferred to a nitrocellulose membrane, and immunoblotted with pp65 antibody to confirm pulldown from interacting with cGAS. Actin was used to confirm equal loading of input. (A–C) $n = 3$.

We next tested if additional viral proteins are required for the interaction of pp65 and cGAS by immunoprecipitating cGAS with WT-pp65 and all nitrosylation-deficient mutants. To determine if wild-type and mutant pp65 proteins can still interact with host-encoded cGAS, NuFF-1 pp65 expressing cells were lysed with Co-IP lysis buffer, and

the immunoprecipitation was repeated as above. In the absence of other viral factors, we observed a robust interaction with cGAS and wild-type pp65, as well as each of the protein-S-nitrosylation deficient mutants (Fig. 5B). These data suggest that blocking protein S-nitrosylation of pp65 has little impact on its interaction with cGAS, and the ability of the DM-pp65 virus to show increased replication in the presence of activated cGAS is likely due to a different effect than interaction with cGAS.

HCMV pp65 interacts with cGAS, thereby inhibiting its capability to produce 2'3'-cGAMP, reducing STING activation (26). Defining if this interaction occurs when the nitrosylation of pp65 is blocked would explain the increased replication of DM-pp65 in the presence of G3-YSD. NuFF-1 cells were infected with WT, SM1-pp65, SM2-pp65, or DM-pp65 expressing HCMV at an MOI of 1 for 72 h. SM1-pp65 and SM2-pp65 are viral mutants, in which only one of the two identified protein-S-nitrosylated cysteines was mutated to a serine, so these viruses can still be protein-S-nitrosylated at one site. Cells were lysed at 72 h, and 50 µg of protein was incubated with anti-cGAS coupled beads. Immunoblotting of the IP revealed bands of equal protein densities for all pp65 mutants (Fig. 5C), suggesting that the protein-S-nitrosylation status of pp65 did not alter the ability of the viral protein to interact with cGAS.

DM-pp65 antagonizes cGAS with better efficiency than wild-type pp65 in stable cell lines

To identify the optimal concentration of G3-YSD for transfection, NuFF-1 parental cells were transfected with various concentrations of G3-YSD, and cell lysates were collected at 4 h post-transfection. Following western blotting, we observed an optimal concentration of 0.2 µg of G3-YSD (Fig. 6A). This concentration was used for the transfection of stable cell lines expressing WT and DM-pp65. To understand if DM-pp65 inhibits cGAS activation to a different level than that of the wild-type protein, stable cell lines expressing either WT or DM-pp65 were transfected with the cGAS activator, G3-YSD, and cell lysates were collected at 2 and 4 h post-transfection. As expected, there was an increase in the levels of phosphorylation of IRF3 and TBK1 in the parental cell lines and a decrease in the phosphorylation status of both proteins in the presence of WT pp65. Importantly, in the DM-pp65 expressing NuFF-1 cells, there was a reduction of phosphorylated IRF3 and TBK1 levels when compared to WT expressing pp65 NuFF-1 cells (Fig. 6B and C). This decrease in phosphorylation suggests that this would result in a decrease in downstream antiviral factors, such as the secretion of IFN-β1. To determine if there are changes in IFN-β1 secretion, stable cell lines were transfected with 0.2 µg of G3-YSD, and then the supernatant was collected 8 h post-treatment to be analyzed by enzyme-linked immunosorbent assay (ELISA). The cell line expressing DM-pp65 group showed a significant decrease in the secretion of IFN-β1 post G3-YSD treatment compared to parental or WT pp65 expressing cell lines (Fig. 6D). Our data reveal that protein-S-nitrosylation-deficient pp65 antagonizes cGAS with better efficiency and leads to a decrease in phosphorylation of IRF3 and TBK1 and a reduction in IFN-β1 secretion. The protein-S-nitrosylation of viral proteins like pp65, coupled with our earlier findings with pp71, suggests that this modification may function as a broadly neutralizing mechanism in HCMV infection.

DISCUSSION

Using mass spectrometry-based proteomics, we identified 13 viral proteins in HCMV infection to be protein-S-nitrosylated. We reported that when protein-S-nitrosylation of pp71 is inhibited, it results in an increased antagonization of the STING pathway compared to WT pp71, thus suggesting the PTM blocks functions of the viral protein. We wanted to understand if this PTM may serve as a universal anti-viral mechanism and not just the inhibition of one specific viral protein. Herein, we focused on identifying the impact of protein-S-nitrosylation of pp65, as our MS/MS analysis identified this critical HCMV protein to be nitrosylated at two independent cysteines, and pp65 inhibits the cytosolic DNA sensor cGAS, a key activator of STING. We observed that by 48 hpi, pp65 is

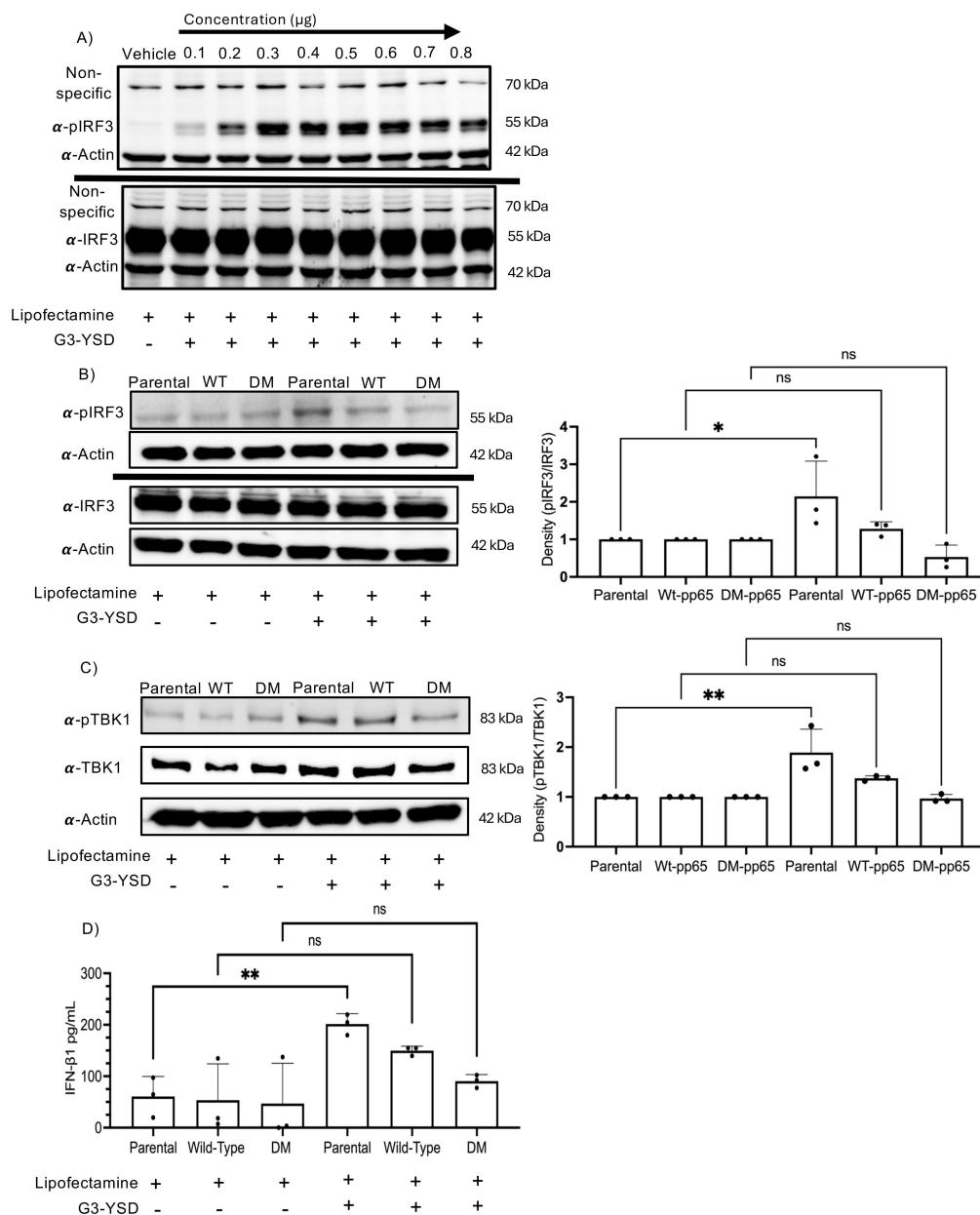


FIG 6 The presence of DM-pp65 in NuFF-1 cells decreases the phosphorylation of pIRF3 and TBK1 after G3-YSD treatment. (A) NuFF-1 cells were transfected with 0.1 to 0.8 µg of G3-YSD. Cell lysates were collected after 4 h post-transfection, and protein lysates were separated by 8% SDS-PAGE. Membranes were then immunoblotted with pIRF3 or IRF3 antibody in two separate blots. (B) NuFF-1 and stable cells were transfected with 0.2 µg of G3-YSD for 4 h, and then cell lysates were collected and processed. Blots were probed with anti-IRF3 and pIRF3. (C) NuFF-1 parental and stable cells were transfected with 0.2 µg of G3-YSD or vehicle for 2 h, and cell lysates were collected and processed. Protein lysates were immunoblotted with anti-TBK1 and pTBK1, and then multiplexed with fluorescent secondary antibodies. (D) NuFF-1 parental and stable cell lines were transfected with 0.2 µg of G3-YSD for 8 h, and then supernatant was collected. Supernatant was then analyzed for IFN-β1 secretion by ELISA. OD readings were read at 450 nm. (A–D) $n = 3$, $P < 0.05^*$, and $P < 0.01^{**}$.

protein-S-nitrosylated. Robust protein expression of pp65 begins at 24 hpi, but we did not observe significant levels of protein-S-nitrosylation of pp65 accumulating at this earlier time point (Fig. 1B and C), suggesting that this modification may be an induced response to viral infection.

Site-directed mutagenesis with BAC recombineering is an important technique allowing one to change specific amino acids in a protein in order to study specific

phenotypes. Two sites identified to be protein-S-nitrosylated within pp65 were changed from cysteines to the structurally similar serine in order to understand the biological impact where pp65 protein-S-nitrosylation is blocked. Often mutating a critical protein may cause a growth defect in viral replication, as it may impact key functions of the protein. A single-step growth curve comparing the replications of WT, DM-pp65, and a revertant virus, in which the mutation was reverted back to the wild-type cysteines, did not reveal a growth disadvantage for the DM-pp65 virus as it grew with similar kinetics as the WT and Rev HCMV, suggesting that the induced mutations in pp65 did not impact lytic replication in fibroblasts (Fig. 2A and B). As mutations can alter the folding and/or turnover of a protein, we wanted to evaluate the integrity of pp65 protein expression. No difference was observed in pp65 protein expression between the WT and DM-pp65 viruses produced in NuFF-1 cells. However, another important function of pp65 is the loading of viral tegument.

The loading of HCMV proteins like UL25, 41, 43, and 71 is reliant on the expression of pp65 (48). The incorporation of proteins into a virion like UL69 and 97 also is impacted by the expression of pp65 (49). Since two sites of pp65 were mutated, we next investigated if the loading of the tegument is impacted. NuFF-1 cells infected with WT and DM-pp65 at an MOI of 1 had no difference in the loading of pp65 within the tegument (Fig. 2C), but it remains to be determined if tegument-delivered pp65 is nitrosylated, a prospect that is difficult due to protein quantities, however. Determining if the protein-S-nitrosylation status of pp65 impacts the loading of other proteins also remains unknown and warrants further investigation. However, as there was no impact on viral lytic replication, this prospect seems unlikely at least for fibroblast infections.

Although the viruses replicate in a similar manner, our focus shifted to investigate if the protein-S-nitrosylation status of pp65 alters its biological functions in attenuating host antiviral responses. We tested the hypothesis that DM-pp65 exhibits a growth advantage in an induced anti-viral state, such as activating cGAS. To this end, fibroblast cells were pre-stimulated with a synthetic double-stranded DNA molecule, G3-YSD, that stimulates cGAS activity prior to infection with either WT or DM-pp65 virus. Under these conditions, WT HCMV replication was attenuated by G3-YSD treatment (Fig. 3B and C). Importantly, and in support of our model, we observed that DM-pp65 still replicated efficiently, even in the presence of an induced anti-viral state (Fig. 3C). Although higher levels of G3-YSD treatment did significantly reduce cell viability, treatments with 0.4 and 0.8 μ g of G3-YSD did not show measurable defects in cell viability, and the mutant virus was still resistant in these treatment groups, whereas WT HCMV was impeded. It is unlikely that cGAS activation is impacting viral entry into fibroblasts, as we still observe mCherry expression in the infected cells, as the viruses contain this fluorescent reporter allowing one to monitor infection. Our data suggest that viral exit and egress are impacted, as there is a decrease in virion production. While we have not investigated the exact viral lifecycle stage that this inhibition of WT virus occurs, it is probable that replication is reduced due to the upregulation of ISGs that inhibit viral replication like IFI16, IFIT1, ISG15, or Mx1 (50–54).

A common technique to inhibit the anti-viral state within a cell is for the virus to target immune effectors responsible for limiting viral replication. We wanted to determine if cGAS is degraded in DM-pp65 HCMV infection and if so, what mechanisms lead to the degradation of cGAS compared to WT HCMV infection. Interestingly, no degradation of cGAS was observed at any of the time points of HCMV infection in our study (Fig. 4). If DM-pp65 degraded cGAS with better efficiency than the WT, we would expect to observe a decrease in interferon production from the absence of cellular cGAS and not a reduced activity of cGAS. Concurrent with our results, the Biolatti Laboratory, which discovered pp65 as a restriction factor for cGAS, also observed no degradation of cGAS, and our previous work identified that infection with WT HCMV does not degrade STING (26, 40). This suggests that the pro-viral phenotype we observe when protein-S-nitrosylation is blocked is not due to the degradation of cGAS or STING, but through a

different mechanism, such as protein-S-nitrosylation impacting pp65's interaction with cGAS.

To further understand the impact of protein-S-nitrosylation on pp65 in HCMV infection, we determined if DM-pp65 demonstrates altered binding to cGAS compared to WT pp65 and if pp65 is protein-S-nitrosylated in the absence of infection. We first observed that in stable cell lines, WT-pp65 is still protein-S-nitrosylated without the presence of other viral factors and without an induced anti-viral state (5A). Biolatti *et al.* reported that pp65 immunoprecipitated with cGAS within protein lysates collected from infection of primary dermal fibroblasts (26, 40). We observed a similar interaction in our work as well, with stable cell lines expressing pp65 and mutant virus (Fig. 5B and C). Interestingly, we found that the nitrosylation-deficient pp65 mutants also immunoprecipitated with cGAS to similar levels as WT virus infection. A possibility remains that DM-pp65 may lead to a reduction in 2'3'-cGAMP production through reduced enzymatic activity, which cannot be measured by Co-IPs, and commercial ELISA kits are highly variable in the recognition of 2'3'-cGAMP within cells and remain a challenge. Furthermore, there remains value in testing if the interaction with other cellular innate proteins is impacted by DM-pp65. For example, pp65 inhibits IFI16 and blocks it from bringing DNA to cGAS to produce 2'3'-cGAMP (55, 56). This could explain why we see no significant alterations in the interaction between cGAS and DM-pp65 but still see a robust replication of virus expressing DM-pp65 after the cGAS/STING pathway is induced.

Next, we tested the biological impact of protein S-nitrosylation of pp65 on downstream antiviral factors of the STING pathway. The stable cell lines were transfected with G3-YSD to induce an anti-viral state inducing canonical cGAS activity. The phosphorylation status of TBK1 and IRF3 was measured and revealed a strong phosphorylation of IRF3 in our parental cells but a decrease of phosphorylation in the infected cells, importantly, with DM-pp65 having a lower level of pIRF3 and pTBK1 when compared to WT (Fig. 6B and C). The total protein levels for IRF3, TBK1, and actin were consistently the same, indicating that the reduction in phosphorylation was from a mechanism upstream of these factors, such as cGAS inhibition. The reduction of TBK1 and IRF3 phosphorylation suggested that DM-pp65 is sufficient to inhibit cGAS, expressing a phenotype where a nitrosylation-deficient pp65 has an increased ability to antagonize cGAS. If DM-pp65 influences the phosphorylation of different signaling molecules like NF- κ B, which pp65 is known to inhibit, remains unknown and will be a focus of future investigations (57).

The phosphorylation of transcription factors like IRF3 leads to the activation of promoters producing cytokines like IFN- β 1 and IL-1 β . This led us to hypothesize that the reduced level of phosphorylation of IRF3 in the DM-pp65 stable cell lines would lead to a reduction in cytokine secretion. In fact, the DM-pp65 expressing stable cell lines had the lowest amount of IFN- β 1 secretion post-G3-YSD treatment, indicating that protein-S-nitrosylation of pp65 has a biological impact in reducing the activity of pp65 in attenuating the cGAS/STING pathway (Fig. 6D). The secretion of IFN- β 1 is important in activating dendritic cells, which will then activate CD4⁺ T-cells initiating the production of antibodies by B-cells (58–61). IFN- β 1 can also activate natural killer cells, which are important in controlling the reactivation of HCMV (62–65). Our results support a model, in which protein-S-nitrosylation of viral virulence factors may function as an intrinsic defense mechanism that may assist in more specific antiviral responses like the secondary immune response in viral infections.

Data from this work and from Nukui *et al.* suggest that protein-S-nitrosylation of HCMV viral proteins may serve as a more universal anti-viral mechanism (40). The exact factors that promote pp65 and pp71 nitrosylation remain unknown, but nitric oxide, the substrate for protein-S-nitrosylation within HCMV infected cells, has been suggested to have anti-viral properties. When nitric oxide donors like DETA-NONO are provided *in trans* to HCMV-infected cells, viral DNA synthesis is inhibited (66). Highlighting the specificity of this response, when HCMV-infected cells are treated with both DETA-NONO and nitric oxide scavenger cPTIO, viral DNA synthesis returns to normal levels, suggesting

that the global removal of nitric oxide groups has a pro-viral mechanism (66). Nitric oxide donors also reduce the spread of HCMV infection in neural organoids, highlighting how potent nitric oxide is in inhibiting HCMV infection in other organs of an infected host (67). Nitric oxide did, however, disrupt the differentiation of neural progenitor cells, indicating this treatment may not be appropriate for use in congenital HCMV infections. We currently do not yet understand why pp65 would conserve this specific amino acid sequence, as our data suggest when protein-S-nitrosylation is blocked, pp65 antagonizes the cGAS/STING pathway with better efficiency. It may be that a nitrosylated pp65 is important in maintaining latency or is required to interact with other proteins within the cell, which we have not investigated yet. These specific cystines may also be important in forming disulfide bridges within the folding of the protein, but we think this is unlikely, as the protein still functions with the introduced mutations. Furthermore, we observed potent protein-S-nitrosylation of pp65 at later times during infection, whereas one could envision that this host-directed modification would need to be induced earlier for maintaining cGAS/STING induction. It is not possible to determine the nitrosylation status of tegument-delivered pp65 due to available protein levels needed for the biotin switch assay. However, one can envision that an infected cell may promote loading of nitrosylated pp65 into newly generated viral progeny so as to limit subsequent infections.

Overall, our work identifies an additional viral protein that is regulated by protein-S-nitrosylation in the cGAS/STING pathway in HCMV infection. We found that blocking protein-S-nitrosylation of pp65 induces a larger decrease in the phosphorylation of IRF3 and TBK1, leading to a decrease in the secretion of IFN- β 1 (Fig. 7). We also observed that DM-pp65 is more resistant to an induced anti-viral state in NuFF-1 cells. Identifying proteins that regulate HCMV infection by protein-S-nitrosylation is important, as these factors may be exploited to develop broadly neutralizing anti-viral therapeutics for HCMV infection and potentially other viruses that encode critical proteins, which are nitrosylated. Furthermore, utilizing nitrosylation-inducing methodologies in a therapeutic manner may provide clinicians with techniques in controlling unmanageable drug-resistant viral infections. In summary, our work suggests that protein-S-nitrosylation functions as an antiviral mechanism that could have potentially broad antiviral effects.

MATERIALS AND METHODS

Cell culture

Newborn fetal fibroblasts (NuFF-1) and phoenix cells were maintained in Dulbecco's Modified Essential Medium (Cleveland Clinic) supplemented with 10% fetal bovine serum (FBS) (Millipore-Sigma), 1% penicillin-streptomycin solution (Cleveland Clinic), and 2 mM L-glutamine (Cleveland Clinic). All incubators were maintained at 5% carbon dioxide at 37°C. Cells infected with HCMV for the expansion of the virus were supplemented with complete medium that instead of FBS contains 10% newborn calf serum (Gibco). All cells were split with 0.5% Trypsin/EDTA (Cleveland Clinic) at a dilution of 1:2, and fibroblast passages were recorded to limit cellular senescence and limited to no more than 30 passages for experiments.

Virus propagation

HCMV genomes are contained in bacterial artificial chromosomes (BAC) in SW105 bacteria. For isolation of HCMV BACs, bacteria are streaked onto Luria Broth (LB) agar-chloramphenicol plate and grew at 32°C for 24 h. The bacteria are then cultured overnight in LB-chloramphenicol broth, and the next day, BAC DNA is isolated and transfected with electroporation into MRC5 cells that are at a 50% confluency. The next day, media are changed on MRC5 cells with complete medium and cultured until the plate is at a 100% cytopathic effect. The virus is then isolated by collecting the supernatant and cells, sonicating, and centrifuging the virus at 20,000 RPM for 1.5 h at 18°C in a 20%

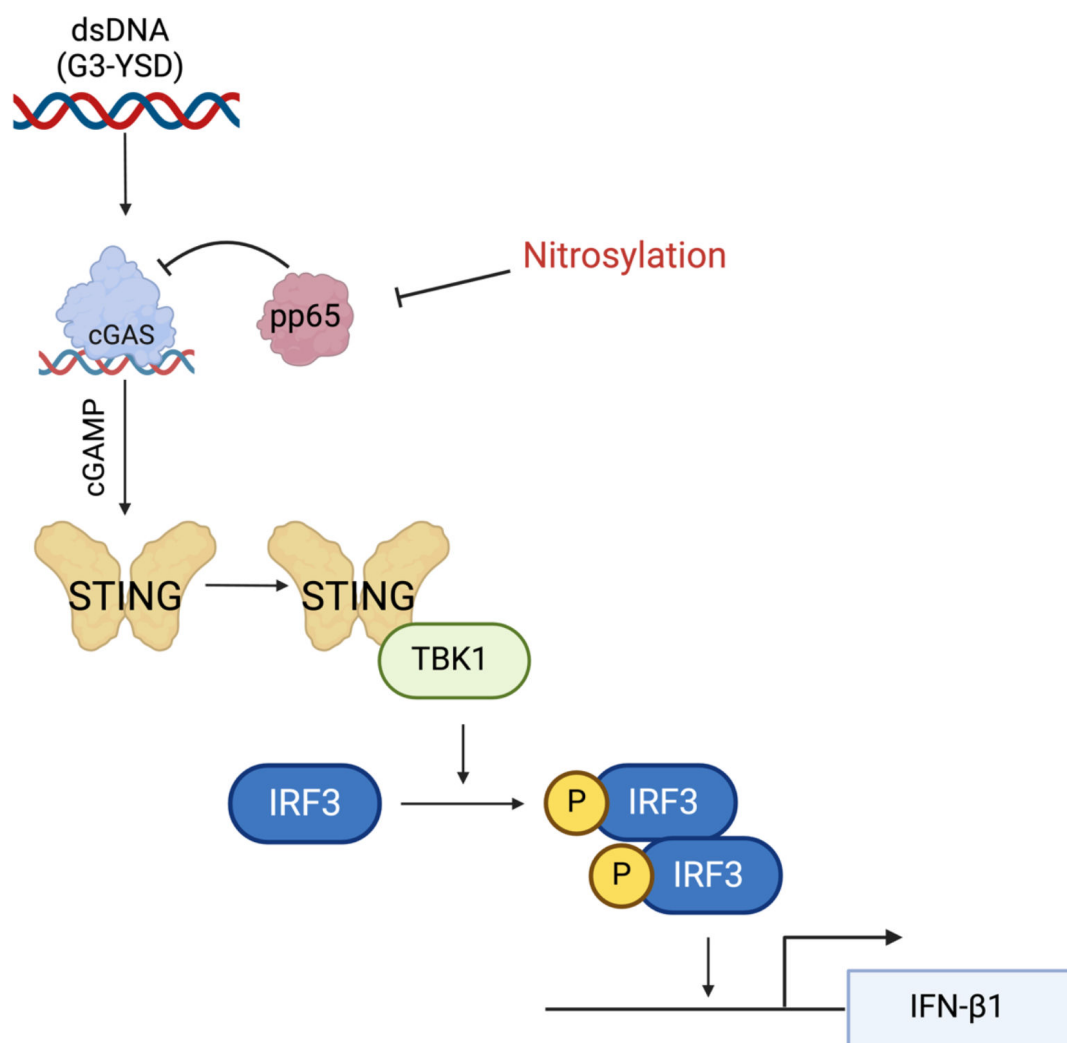


FIG 7 The nitrosylation of pp65 is an antiviral mechanism limiting its ability to inhibit cGAS. Our data suggest that when nitrosylation of pp65 is blocked, it has a better ability to antagonize cGAS, as observed by a decrease in phosphorylation of IRF3 and TBK1 in the presence of the DM-pp65 mutant protein. This decrease in IRF3 phosphorylation led to a decrease in IFN-β1 secretion. We report that DM-pp65 is resistant to cGAS activation in NuFF-1 cells, resulting in increased replication during STING activation compared to WT virus. Created in BioRender. Cox, J. (2025) <https://BioRender.com/b57t258>.

sorbitol cushion with an SW-28 rotor in a Beckman Coulter ultracentrifuge. The virus is then titered by TCID₅₀ to measure PFU/mL.

Retroviral production and transduction

Phoenix cells were seeded at 80% confluency a day before transfection. To form DNA:lipofectamine complexes, 1 µg of retroviral plasmid pLXSN-pp65 WT or DM was incubated with 10 µL of Lipofectamine 2000 (Thermo Fisher) in Opti-MEM for 30 min at room temperature. DNA:lipofectamine complexes were overlaid onto Phoenix cells overnight, and the following day, media were changed to 10% NCS supplemented with 2 mM L-glutamine. The supernatant was collected at 48 and 72 h post-media change, filtered with a 0.45 µm filter (Sigma) and media overlaid on NuFF-1 cells at 70% confluency. NuFF-1 cells were then selected with 300 µg/mL of G-418 (Invitrogen) and allowed to grow for two doublings. Protein expression was confirmed with western blot.

G3-YSD transfection

G3-YSD was transfected at various concentrations, as indicated in the Results section. Lipofectamine 2000 (Thermo Fisher) was incubated with G3-YSD for 30 min at room temperature in Opti-Mem to allow complexes to form. After incubation, complexes were added to NuFF-1 cells at 75% confluency dropwise and incubated for 2, 4, or 24 h post-transfection depending on the experiment.

Measuring viral titers

Human cytomegalovirus is titered by TCID₅₀ assay. NuFF-1 cells are seeded to 90% confluency in a 96-well plate 24 h prior to infection. Viral supernatant is serially diluted 1:10, and viral plaques are counted 14 dpi by visualization of mCherry expression.

Western blotting and co-immunoprecipitation

Protein was isolated by scraping cells with 100 μ L of Pierce RIPA lysis and extraction buffer (25 mM Tris-HCl pH 7.6, 150 mM NaCl, 1% NP-40, 1% sodium deoxycholate, 0.1% SDS; Thermo Fisher Scientific). Lysates were incubated on ice for 30 min and sonicated 2 \times for 15 s to lyse cells. Lysates were quantitated by Bradford assay, and 30 μ g of protein was separated with 8% SDS-PAGE. Following separation, protein was transferred to a nitrocellulose membrane and blocked with 5% BSA for 1 h at room temperature. The membranes were probed with anti-pp65 (1:200, 8A8), anti-cGAS (1:1,000, Sigma), hFAB rhodamine anti-GAPDH (1:5,000, Bio-Rad), anti-actin (1:10,000, Cell Signaling), anti-pIRF3 (1:500, 4D4G, Cell Signaling), anti-IRF3 (1:2,000, Cell Signaling), anti-pTBK1 (1:500, D52C2, Cell Signaling), and anti-TBK1 (1:500, E9H5S, Cell Signaling) overnight at 4°C, and then washed with TBS-Tween (0.1%) the following day three times for 5 min each wash. Secondary antibodies anti-mouse or rabbit-HRP (1:2,000, Cell Signaling) were probed for 1 h at room temperature, and then washed an additional three times for 5 min each wash. All images were processed and imaged on Bio-Rad's Chemidoc with chemiluminescence or by fluorescence.

Co-immunoprecipitation experiments were lysed with Pierce Co-IP lysis buffer (25 mM Tris-HCl pH 7.4, 150 mM NaCl, 1 mM EDTA, 1% NP-40, and 5% glycerol, Thermo Fisher Scientific) containing Pierce protease and phosphatase tablet inhibitor mini-tablets, EDTA-free (Thermo Fisher Scientific). Next, 100 μ g of protein was incubated with anti-cGAS (1:50) overnight, and the following day, was incubated with anti-rabbit DynaBeads (Thermo Fisher Scientific), and then incubated 2 h at 4°C. The following day, samples were washed five times with Co-IP lysis buffer, and beads were boiled for 5 min in 2 \times Laemmli buffer, and then separated on 8% SDS-PAGE, transferred to a nitrocellulose membrane, and blocked with 5% BSA. Membranes were probed with anti-cGAS (1:1,000) or anti-pp65 (1:200) antibody overnight at 4°C. The following day, samples were probed with respective secondary antibodies, and membranes were developed in chemiluminescent buffer and imaged on a Bio-Rad ChemiDoc.

Biotin capture of nitrosylated proteins

Accordingly, 100 μ g of protein from HCMV-infected cell lysates was subjected to a biotin switch assay following manufacturer protocol (Cayman Chemical Company). Biotinylated proteins were affinity-purified with streptavidin-coated M-280 Dynabeads (Thermo Fisher Scientific) overnight and washed six times with cold PBS using Life Technologies Dynamag-2. Beads were boiled in 2 \times Laemmli and loaded onto an 8% SDS-PAGE. Protein was separated and probed for antibodies specific to HCMV pp65.

IFN- β 1 ELISA

Cytokine secretion was measured using the VeriKine Human IFN Beta ELISA Kit from PBL Assay Science. Parental and pp65 expressing stable cell lines were transfected with 0.2 μ g of G3-YSD for 8 h in Opti-MEM. Media were collected and clarified, and 50 μ L

of supernatant was added to respective wells and incubated for 1 h at room temperature. Wells were washed three times with ELISA wash buffer (TBS 0.05% Tween-20) and liquid aspirated from wells. Antibody from the kit was diluted 1:150, and the antibody solution was added to wells and incubated for 1 h at room temperature. Wells were then washed again as stated before, and HRP-conjugated secondary antibody was diluted 1:100 and added to wells for 1 h at room temperature. After another three washes, TMB substrate was added to the wells and allowed to develop for 15 min in the dark at room temperature. Once the ELISA plate fully developed, stop solution was added to each well, and absorbance was measured at 450 nm. Cytokine measurement was quantified by calculating pg/mL of IFN- β 1 in the supernatant using the equation provided by the standard curve.

Statistics

All experiments in this paper were analyzed using unpaired Student's *t*-test. Results were considered significant if the calculated *P*-value was < 0.05 indicated by a 95% CI. All data were graphed and analyzed utilizing the program GraphPad Prism.

ACKNOWLEDGMENTS

We are grateful for Masatoshi Nukui for developing reagents for this project and initial work on discovering that HCMV proteins are protein-S-nitrosylated in HCMV infection. We thank Zsuzsa Szemere Ph.D., Meghan Carter, Emmanuel Ijeize Ph.D., and Mary Root for their technical support and scientific advice.

E.A.M. acknowledges support from the National Institutes of Health (award no. 5R01AI155979-04).

J.B.C. and E.A.M. contributed to the theory of the study. J.B.C. performed experiments. J.B.C. and E.A.M. analyzed and interpreted the data. M.N. developed reagents, such as stable cell lines and viruses. J.B.C. wrote the initial draft of this manuscript. J.B.C. and E.A.M. reviewed and edited the manuscript.

AUTHOR AFFILIATION

¹Microbiology and Immunology Department, SUNY Upstate Medical University, Syracuse, New York, USA

AUTHOR ORCIDs

Justin B. Cox  <http://orcid.org/0000-0003-3095-1512>

Eain A. Murphy  <http://orcid.org/0000-0003-3449-5024>

FUNDING

Funder	Grant(s)	Author(s)
National Institute of Allergy and Infectious Diseases	R01AI155979	Eain A. Murphy
National Institute on Aging	R01AG076007	Eain A. Murphy

AUTHOR CONTRIBUTIONS

Justin B. Cox, Conceptualization, Data curation, Formal analysis, Methodology, Resources, Writing – original draft, Writing – review and editing | Eain A. Murphy, Conceptualization, Formal analysis, Funding acquisition, Project administration, Supervision, Writing – review and editing.

DATA AVAILABILITY

The authors will make all data and reagents generated and described in this paper available to the scientific community upon request.

REFERENCES

- Sijmons S, Van Ranst M, Maes P. 2014. Genomic and functional characteristics of human cytomegalovirus revealed by next-generation sequencing. *Viruses* 6:1049–1072. <https://doi.org/10.3390/v6031049>
- Van Damme E, Van Loock M. 2014. Functional annotation of human cytomegalovirus gene products: an update. *Front Microbiol* 5:218. <https://doi.org/10.3389/fmicb.2014.00218>
- Scrivano L, Sinzger C, Nitschko H, Koszinowski UH, Adler B. 2011. HCMV spread and cell tropism are determined by distinct virus populations. *PLoS Pathog* 7:e1001256. <https://doi.org/10.1371/journal.ppat.1001256>
- O'Connor CM, Murphy EA. 2012. A myeloid progenitor cell line capable of supporting human cytomegalovirus latency and reactivation, resulting in infectious progeny. *J Virol* 86:9854–9865. <https://doi.org/10.1128/JVI.01278-12>
- Griffiths P, Reeves M. 2021. Pathogenesis of human cytomegalovirus in the immunocompromised host. *Nat Rev Microbiol* 19:759–773. <https://doi.org/10.1038/s41579-021-00582-z>
- Tomtishen J. 2012. Human cytomegalovirus tegument proteins (pp65, pp71, pp150, pp28). *Virology* 9:22. <https://doi.org/10.1186/1743-422X-9-22>
- Sun L, Chen J-M, Yang K, Zhang L, Ma Z-Y, Chen X-M, Li M, Zhou X, Li P, Zhao H-X, Xiao J, Qi L-M, Wang P. 2022. Cytomegalovirus cell tropism and clinicopathological characteristics in gastrointestinal tract of patients with HIV/AIDS. *Diagn Pathol* 17:9. <https://doi.org/10.1186/s13000-022-01193-9>
- Jakharia N, Howard D, Riedel DJ. 2021. CMV infection in hematopoietic stem cell transplantation: prevention and treatment strategies. *Curr Treat Options Infect Dis* 13:123–140. <https://doi.org/10.1007/s40506-021-00253-w>
- Carlson A, Norwitz ER, Stiller RJ. 2010. Cytomegalovirus infection in pregnancy: should all women be screened? *Rev Obstet Gynecol* 3:172–179.
- Erice A. 1999. Resistance of human cytomegalovirus to antiviral drugs. *Clin Microbiol Rev* 12:286–297. <https://doi.org/10.1128/CMR.12.2.286>
- Boivin G, Goyette N, Rollag H, Jardine AG, Pescovitz MD, Asberg A, Ives J, Hartmann A, Humar A. 2009. Cytomegalovirus resistance in solid organ transplant recipients treated with intravenous ganciclovir or oral valganciclovir. *Antivir Ther* 14:697–704.
- Zhang X, Shi H, Wu J, Zhang X, Sun L, Chen C, Chen ZJ. 2013. Cyclic GMP-AMP containing mixed phosphodiester linkages is an endogenous high-affinity ligand for STING. *Mol Cell* 51:226–235. <https://doi.org/10.1016/j.molcel.2013.05.022>
- Gao P, et al. 2013. Cyclic [G(2',5')pA(3',5')p] is the metazoan second messenger produced by DNA-activated cyclic GMP-AMP synthase. *Cell* 153:1094–1107. <https://doi.org/10.1016/j.cell.2013.04.046>
- Ablasser A, Goldeck M, Cavlar T, Deimling T, Witte G, Röhl I, Hopfner K-P, Ludwig J, Hornung V. 2013. cGAS produces a 2'-5'-linked cyclic dinucleotide second messenger that activates STING. *Nature* 498:380–384. <https://doi.org/10.1038/nature12306>
- Diner EJ, Burdette DL, Wilson SC, Monroe KM, Kellenberger CA, Hyodo M, Hayakawa Y, Hammond MC, Vance RE. 2013. The innate immune DNA sensor cGAS produces a noncanonical cyclic dinucleotide that activates human STING. *Cell Rep* 3:1355–1361. <https://doi.org/10.1016/j.jcelrep.2013.05.009>
- Li X, Shu C, Yi G, Chaton CT, Shelton CL, Diao J, Zuo X, Kao CC, Herr AB, Li P. 2013. Cyclic GMP-AMP synthase is activated by double-stranded DNA-induced oligomerization. *Immunity* 39:1019–1031. <https://doi.org/10.1016/j.immuni.2013.10.019>
- Wang Y-Y, Liu L-J, Zhong B, Liu T-T, Li Y, Yang Y, Ran Y, Li S, Tien P, Shu H-B. 2010. WDR5 is essential for assembly of the VISA-associated signaling complex and virus-triggered IRF3 and NF- κ B activation. *Proc Natl Acad Sci USA* 107:815–820. <https://doi.org/10.1073/pnas.0908967107>
- Jin L, Waterman PM, Jonscher KR, Short CM, Reisdorph NA, Cambier JC. 2008. MPY5, a novel membrane tetraspanner, is associated with major histocompatibility complex class II and mediates transduction of apoptotic signals. *Mol Cell Biol* 28:5014–5026. <https://doi.org/10.1128/MCB.00640-08>
- Sun W, Li Y, Chen L, Chen H, You F, Zhou X, Zhou Y, Zhai Z, Chen D, Jiang Z. 2009. ERIS, an endoplasmic reticulum IFN stimulator, activates innate immune signaling through dimerization. *Proc Natl Acad Sci USA* 106:8653–8658. <https://doi.org/10.1073/pnas.0900850106>
- Ishikawa H, Barber GN. 2008. STING is an endoplasmic reticulum adaptor that facilitates innate immune signalling. *Nature* 455:674–678. <https://doi.org/10.1038/nature07317>
- Zhong B, Yang Y, Li S, Wang Y-Y, Li Y, Diao F, Lei C, He X, Zhang L, Tien P, Shu H-B. 2008. The adaptor protein MITA links virus-sensing receptors to IRF3 transcription factor activation. *Immunity* 29:538–550. <https://doi.org/10.1016/j.immuni.2008.09.003>
- Paijo J, Döring M, Spanier J, Grabski E, Nooruzzaman M, Schmidt T, Witte G, Messerle M, Hornung V, Kaever V, Kalinke U. 2016. cGAS senses human cytomegalovirus and induces type I interferon responses in human monocyte-derived cells. *PLoS Pathog* 12:e1005546. <https://doi.org/10.1371/journal.ppat.1005546>
- Lam E, Stein S, Falck-Pedersen E. 2014. Adenovirus detection by the cGAS/STING/TBK1 DNA sensing cascade. *J Virol* 88:974–981. <https://doi.org/10.1128/JVI.02702-13>
- Reinert LS, Lopusná K, Winther H, Sun C, Thomsen MK, Nandakumar R, Mogensen TH, Meyer M, Vægter C, Nyengaard JR, Fitzgerald KA, Paludan SR. 2016. Sensing of HSV-1 by the cGAS-STING pathway in microglia orchestrates antiviral defence in the CNS. *Nat Commun* 7:13348. <https://doi.org/10.1038/ncomms13348>
- Malouli D, Hansen SG, Nakayasu ES, Marshall EE, Hughes CM, Ventura AB, Gilbride RM, Lewis MS, Xu G, Kreklywich C, Whizin N, Fischer M, Legasse AW, Viswanathan K, Siess D, Camp DG 2nd, Axthelm MK, Kahl C, DeFilippis VR, Smith RD, Streblow DN, Picker LJ, Früh K. 2014. Cytomegalovirus pp65 limits dissemination but is dispensable for persistence. *J Clin Invest* 124:1928–1944. <https://doi.org/10.1172/JCI67420>
- Biolatti M, Dell'Oste V, Pautasso S, Gugliesi F, von Einem J, Krapp C, Jakobsen MR, Borgogna C, Gariglio M, De Andrea M, Landolfo S. 2018. Human Cytomegalovirus tegument protein pp65 (pUL83) dampens type I interferon production by inactivating the DNA sensor cGAS without affecting STING. *J Virol* 92:e01774-17. <https://doi.org/10.1128/JVI.01774-17>
- Abate DA, Watanabe S, Mocarski ES. 2004. Major human cytomegalovirus structural protein pp65 (ppUL83) prevents interferon response factor 3 activation in the interferon response. *J Virol* 78:10995–11006. <https://doi.org/10.1128/JVI.78.20.10995-11006.2004>
- Baldick CJ, Shenk T. 1996. Proteins associated with purified human cytomegalovirus particles. *J Virol* 70:6097–6105. <https://doi.org/10.1128/JVI.70.9.6097-6105.1996>
- Oh K-J, Kalinina A, Wang J, Nakayama K, Nakayama KI, Bagchi S. 2004. The papillomavirus E7 oncoprotein is ubiquitinated by UbcH7 and cullin 1- and Skp2-containing E3 ligase. *J Virol* 78:5338–5346. <https://doi.org/10.1128/jvi.78.10.5338-5346.2004>
- Kamio M, Yoshida T, Ogata H, Douchi T, Nagata Y, Inoue M, Hasegawa M, Yonemitsu Y, Yoshimura A. 2004. SOCS1 [corrected] inhibits HPV-E7-mediated transformation by inducing degradation of E7 protein. *Oncogene* 23:3107–3115. <https://doi.org/10.1038/sj.onc.1207453>
- Wu X, Hu Y, Sui C, Pan L, Yoo D, Miller LC, Lee C, Cong X, Li J, Du Y, Qi J. 2022. Multiple-site SUMOylation of FMDV 3C protease and its negative role in viral replication. *J Virol* 96:e0061222. <https://doi.org/10.1128/jvi.00612-22>
- Dawson AR, Wilson GM, Freiburger EC, Mondal A, Coon JJ, Mehle A. 2020. Phosphorylation controls RNA binding and transcription by the influenza virus polymerase. *PLoS Pathog* 16:e1008841. <https://doi.org/10.1371/journal.ppat.1008841>
- Ali H, Mano M, Braga L, Naseem A, Marini B, Vu DM, Collesi C, Meroni G, Lusic M, Giacca M. 2019. Cellular TRIM33 restrains HIV-1 infection by targeting viral integrase for proteasomal degradation. *Nat Commun* 10:926. <https://doi.org/10.1038/s41467-019-08810-0>
- Stomberski CT, Hess DT, Stamler JS. 2019. Protein S-nitrosylation: determinants of specificity and enzymatic regulation of S-nitrosothiol-based signaling. *Antioxid Redox Signal* 30:1331–1351. <https://doi.org/10.1089/ars.2017.7403>
- Nakamura T, Wang L, Wong CCL, Scott FL, Eckelman BP, Han X, Tzitzilonis C, Meng F, Gu Z, Holland EA, Clemente AT, Okamoto S, Salvesen GS, Riek R, Yates JR, Lipton SA. 2010. Transnitrosylation of XIAP regulates caspase-dependent neuronal cell death. *Mol Cell* 39:184–195. <https://doi.org/10.1016/j.molcel.2010.07.002>
- Seth D, Hess DT, Hausladen A, Wang L, Wang Y-J, Stamler JS. 2018. A multiplex enzymatic machinery for cellular protein S-nitrosylation. *Mol Cell* 69:451–464. <https://doi.org/10.1016/j.molcel.2017.12.025>
- Lee DS, Kim JE. 2021. Protein disulfide isomerase-mediated S-nitrosylation facilitates surface expression of P2X7 receptor following status epilepticus. *J Neuroinflammation* 18:14. <https://doi.org/10.1186/s12974-020-02058-y>

38. Cho DH, et al. 1979. β -amyloid-related mitochondrial fission and neuronal injury. *Science* 324:102–105. <https://doi.org/10.1126/science.1171091>
39. Zell R, Markgraf R, Schmidtke M, Görlach M, Stelzner A, Henke A, Sigusch HH, Glück B. 2004. Nitric oxide donors inhibit the coxsackievirus B3 proteinases 2A and 3C in vitro, virus production in cells, and signs of myocarditis in virus-infected mice. *Med Microbiol Immunol* 193:91–100. <https://doi.org/10.1007/s00430-003-0198-6>
40. Nukui M, Roche KL, Jia J, Fox PL, Murphy EA. 2020. Protein S-nitrosylation of human cytomegalovirus pp71 inhibits its ability to limit STING antiviral responses. *J Virol* 94:e00033-20. <https://doi.org/10.1128/JVI.00033-20>
41. García-Ortiz A, Martín-Cofreces NB, Ibiza S, Ortega Á, Izquierdo-Álvarez A, Trullo A, Victor VM, Calvo E, Sot B, Martínez-Ruiz A, Vázquez J, Sánchez-Madrid F, Serrador JM. 2017. eNOS S-nitrosylates β -actin on Cys374 and regulates PKC- θ at the immune synapse by impairing actin binding to profilin-1. *PLoS Biol* 15:e2000653. <https://doi.org/10.1371/journal.pbio.2000653>
42. M. Bansbach H, H. Guilford W. 2016. Actin nitrosylation and its effect on myosin driven motility. *AIMS Mol Sci* 3:426–438. <https://doi.org/10.3934/molsci.2016.3.426>
43. Lu J, Katano T, Uta D, Furue H, Ito S. 2011. Rapid S-nitrosylation of actin by NO-generating donors and in inflammatory pain model mice. *Mol Pain* 7:101. <https://doi.org/10.1186/1744-8069-7-101>
44. Xu X, Qiu H, Shi F, Wang Z, Wang X, Jin L, Chi L, Zhang Q. 2019. The protein S-nitrosylation of splicing and translational machinery in vascular endothelial cells is susceptible to oxidative stress induced by oxidized low-density lipoprotein. *J Proteomics* 195:11–22. <https://doi.org/10.1016/j.jpro.2019.01.001>
45. Schmolke S, Kern HF, Drescher P, Jahn G, Plachter B. 1995. The dominant phosphoprotein pp65 (UL83) of human cytomegalovirus is dispensable for growth in cell culture. *J Virol* 69:5959–5968. <https://doi.org/10.1128/JVI.69.10.5959-5968.1995>
46. Depto AS, Stenberg RM. 1989. Regulated expression of the human cytomegalovirus pp65 gene: octamer sequence in the promoter is required for activation by viral gene products. *J Virol* 63:1232–1238. <https://doi.org/10.1128/JVI.63.3.1232-1238.1989>
47. Geballe AP, Leach FS, Mocarski ES. 1986. Regulation of cytomegalovirus late gene expression: gamma genes are controlled by posttranscriptional events. *J Virol* 57:864–874. <https://doi.org/10.1128/JVI.57.3.864-874.1986>
48. Reyda S, Tenzer S, Navarro P, Gebauer W, Saur M, Krauter S, Büscher N, Plachter B. 2014. The tegument protein pp65 of human cytomegalovirus acts as an optional scaffold protein that optimizes protein uploading into viral particles. *J Virol* 88:9633–9646. <https://doi.org/10.1128/JVI.01415-14>
49. Chevillotte M, Landwehr S, Linta L, Frascaroli G, Lüske A, Buser C, Mertens T, von Einem J. 2009. Major tegument protein pp65 of human cytomegalovirus is required for the incorporation of pUL69 and pUL97 into the virus particle and for viral growth in macrophages. *J Virol* 83:2480–2490. <https://doi.org/10.1128/JVI.01818-08>
50. Kim YJ, Kim ET, Kim Y-E, Lee MK, Kwon KM, Kim KI, Stamminger T, Ahn J-H. 2016. Consecutive inhibition of ISG15 expression and ISGylation by cytomegalovirus regulators. *PLoS Pathog* 12:e1005850. <https://doi.org/10.1371/journal.ppat.1005850>
51. Bianco C, Mohr I. 2017. Restriction of human cytomegalovirus replication by ISG15, a host effector regulated by cGAS-STING double-stranded-DNA sensing. *J Virol* 91:e02483-16. <https://doi.org/10.1128/JVI.02483-16>
52. Griffante G, Gugliesi F, Pasquero S, Dell'Oste V, Biolatti M, Salinger AJ, Mondal S, Thompson PR, Weerapana E, Lebbink RJ, Soppe JA, Stamminger T, Girault V, Pichlmair A, Oroszlán G, Coen DM, De Andrea M, Landolfo S. 2021. Human cytomegalovirus-induced host protein citrullination is crucial for viral replication. *Nat Commun* 12:3910. <https://doi.org/10.1038/s41467-021-24178-6>
53. Zhang L, Wang B, Li L, Qian D-M, Yu H, Xue M-L, Hu M, Song X-X. 2017. Antiviral effects of IFIT1 in human cytomegalovirus-infected fetal astrocytes. *J Med Virol* 89:672–684. <https://doi.org/10.1002/jmv.24674>
54. Gariano GR, Dell'Oste V, Bronzini M, Gatti D, Luganini A, De Andrea M, Gribaudo G, Gariglio M, Landolfo S. 2012. The intracellular DNA sensor IFI16 gene acts as restriction factor for human cytomegalovirus replication. *PLoS Pathog* 8:e1002498. <https://doi.org/10.1371/journal.ppat.1002498>
55. Li T, Chen J, Cristea IM. 2013. Human cytomegalovirus tegument protein pUL83 inhibits IFI16-mediated DNA sensing for immune evasion. *Cell Host Microbe* 14:591–599. <https://doi.org/10.1016/j.chom.2013.10.007>
56. Biolatti M, Dell'Oste V, Pautasso S, von Einem J, Marschall M, Plachter B, Gariglio M, De Andrea M, Landolfo S. 2016. Regulatory Interaction between the cellular restriction factor IFI16 and viral pp65 (pUL83) modulates viral gene expression and IFI16 protein stability. *J Virol* 90:8238–8250. <https://doi.org/10.1128/JVI.00923-16>
57. Browne EP, Shenk T. 2003. Human cytomegalovirus UL83-coded pp65 virion protein inhibits antiviral gene expression in infected cells. *Proc Natl Acad Sci USA* 100:11439–11444. <https://doi.org/10.1073/pnas.1534570100>
58. Longman RS, Braun D, Pellegrini S, Rice CM, Darnell RB, Albert ML. 2007. Dendritic-cell maturation alters intracellular signaling networks, enabling differential effects of IFN- α /beta on antigen cross-presentation. *Blood* 109:1113–1122. <https://doi.org/10.1182/blood-2006-05-023465>
59. Celli S, García Z, Bousso P. 2005. CD4 T cells integrate signals delivered during successive DC encounters in vivo. *J Exp Med* 202:1271–1278. <https://doi.org/10.1084/jem.20051018>
60. Nagai T, Devergne O, Mueller TF, Perkins DL, van Seventer JM, van Seventer GA. 2003. Timing of IFN- β exposure during human dendritic cell maturation and naive Th cell stimulation has contrasting effects on Th1 subset generation: a role for IFN- β -mediated regulation of IL-12 family cytokines and IL-18 in naive Th cell differentiation. *J Immunol* 171:5233–5243. <https://doi.org/10.4049/jimmunol.171.10.5233>
61. Marrack P, Kappler J, Mitchell T. 1999. Type I interferons keep activated T cells alive. *J Exp Med* 189:521–530. <https://doi.org/10.1084/jem.189.3.521>
62. Madera S, Rapp M, Firth MA, Beilke JN, Lanier LL, Sun JC. 2016. Type I IFN promotes NK cell expansion during viral infection by protecting NK cells against fratricide. *J Exp Med* 213:225–233. <https://doi.org/10.1084/jem.20150712>
63. Shang Q-N, Yu X-X, Xu Z-L, Chen Y-H, Han T-T, Zhang Y-Y, Lv M, Sun Y-Q, Wang Y, Xu L-P, Zhang X-H, Zhao X-Y, Huang X-J. 2023. Expanded clinical-grade NK cells exhibit stronger effects than primary NK cells against HCMV infection. *Cell Mol Immunol* 20:895–907. <https://doi.org/10.1038/s41423-023-01046-5>
64. Lopez-Vergès S, Milush JM, Schwartz BS, Pando MJ, Jarjoura J, York VA, Houchins JP, Miller S, Kang S-M, Norris PJ, Nixon DF, Lanier LL. 2011. Expansion of a unique CD57⁺NKG2C^{hi} natural killer cell subset during acute human cytomegalovirus infection. *Proc Natl Acad Sci USA* 108:14725–14732. <https://doi.org/10.1073/pnas.1110900108>
65. Wu Z, Sinzger C, Frascaroli G, Reichel J, Bayer C, Wang L, Schirmbeck R, Mertens T. 2013. Human cytomegalovirus-induced NKG2C(hi) CD57(hi) natural killer cells are effectors dependent on humoral antiviral immunity. *J Virol* 87:7717–7725. <https://doi.org/10.1128/JVI.01096-13>
66. Mokry RL, Schumacher ML, Hogg N, Terhune SS. 2020. Nitric oxide circumvents virus-mediated metabolic regulation during human cytomegalovirus infection. *MBio* 11:e02630-20. <https://doi.org/10.1128/mBio.02630-20>
67. Mokry RL, O'Brien BS, Adelman JW, Rosas S, Schumacher ML, Ebert AD, Terhune SS. 2022. Nitric oxide attenuates human cytomegalovirus infection yet disrupts neural cell differentiation and tissue organization. *J Virol* 96:e0012622. <https://doi.org/10.1128/jvi.00126-22>